AD-A058 336 ARMY COMMAND AND GENERAL STAFF COLL FORT LEAVENWORTH KANS F/G 4/2
MODELED METEOROLOGICAL INPUTS TO ENVIRONMENT DEPENDENT SIMULATI--ETC(U)
JUN 78 D A ABBOTT

UNCLASSIFIED

1 OF

AD
A058 336

NL

END
DATE
FILMED
10-78
DDC

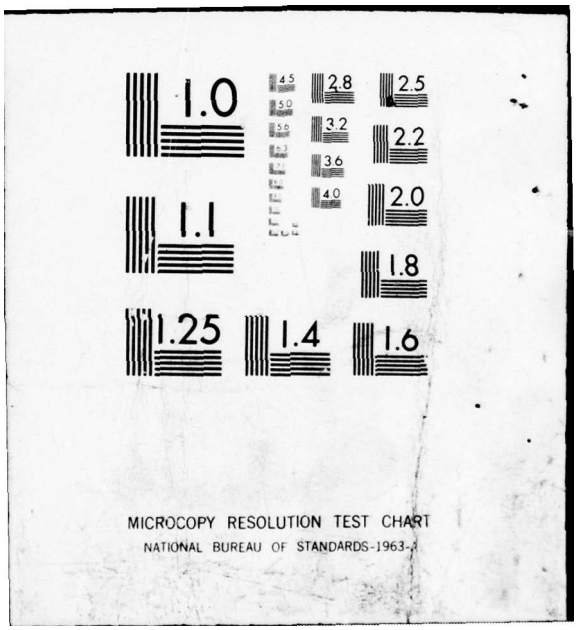
1.0
1.1
1.25
1.4
1.6
1.8
2.0
2.2
2.5
2.8
3.2
3.6
4.0
4.5
5.0
5.6
6.3
MICROCOPY RESOLUTION TEST CHART
NATIONAL BUREAU OF STANDARDS-1963-A

MODELED METEOROLOGICAL INPUTS TO ENVIRONMENT DEPENDENT SIMULATION STUDIES

A thesis presented to the Faculty of the U.S. Army Command and General Staff College in partial fulfillment of the requirements for the degree

MASTER OF MILITARY ART AND SCIENCE

by
Douglas A. Abbott, MAJ, USAF
B.S., Central Michigan University, 1963
M.S., Florida State University, 1969
Ph.D., Florida State University, 1973

Fort Leavenworth, Kansas
1978

SECURITY CLASSIFICATION OF THIS PAGE (When Data Entered)

REPORT DOCUMENTATION PAGE		READ INSTRUCTIONS BEFORE COMPLETING FORM
1. REPORT NUMBER	2. GOVT ACCESSION NO.	3. RECIPIENT'S CATALOG NUMBER
4. TITLE (and Subtitle) MODELED METEOROLOGICAL INPUTS TO ENVIR-ONMENT DEPENDENT SIMULATION STUDIES		5. TYPE OF REPORT & PERIOD COVERED Final Report 9 June 78 6. PERFORMING ORG. REPORT NUMBER
7. AUTHOR(s) ~~Douglas A. Abbott~~ Abbott, Douglas A., MAJ, USAF		8. CONTRACT OR GRANT NUMBER(s)
9. PERFORMING ORGANIZATION NAME AND ADDRESS Student at the U.S. Army Command and General Staff College Fort Leavenworth, KS 66027		10. PROGRAM ELEMENT, PROJECT, TASK AREA & WORK UNIT NUMBERS
11. CONTROLLING OFFICE NAME AND ADDRESS US Army Command and General Staff College ATTN: ATSW-SE		12. REPORT DATE 9 Jun 78 13. NUMBER OF PAGES
14. MONITORING AGENCY NAME & ADDRESS(if different from Controlling Office)		15. SECURITY CLASS. (of this report) Unclassified 15a. DECLASSIFICATION/DOWNGRADING SCHEDULE

16. DISTRIBUTION STATEMENT (of this Report)

Approved for public release; distribution unlimited.

17. DISTRIBUTION STATEMENT (of the abstract entered in Block 20, if different from Report)

Approved for public release; distribution unlimited.

18. SUPPLEMENTARY NOTES

Master of Military Art and Science (MMAS) Thesis prepared at CGSC in partial fulfillment of the Masters Program requirements, U.S. Army Command and General Staff College, Fort Leavenworth, Kansas 66027.

19. KEY WORDS (Continue on reverse side if necessary and identify by block number)

Simulation
Meteorology
Models
Weather
Meteorological Phenomena

20. ABSTRACT (Continue on reverse side if necessary and identify by block number)

A stochastic model demonstrates low-cost meteorological support to environment dependent simulation studies. Only the univariate problem is demonstrated, but extentions to multivariate applications are feasible. This application models atmospheric visibility. The model simulates time series at a given geographical point. A historically derived cumulative frequency distribution is converted to its equivalent normal deviate and fitted by a rational approximation. A Markovian time dependence

DD FORM 1 JAN 73 1473 EDITION OF 1 NOV 65 IS OBSOLETE

SECURITY CLASSIFICATION OF THIS PAGE (When Data Entered)

BLOCK 20 continued:
is assumed. Seasonal and diurnal cycles are modeled. A run is initiated via a random draw from a unit normal distribution. Alternately, an ititial value may be specified. Subsequent values are generated using a time-correlation weighted linear combination of the prior value and a unit normal random input. This produces a Brownian Movement phenomena within the appropriate probability density function. A given run tends to regress toward the climatological mean while exhibiting random fluctuations. A run of sufficient length recreates the probability density functions. Results presented verify model performance against historical data and include a few applications. The FORTRAN subroutine is published in an appendix.

(6) Modeled Meteorological Inputs to Environment Dependent Simulation Studies.

(10) Douglas A. Abbott, MAJ, USAF
U.S. Army Command and General Staff College
Fort Leavenworth, Kansas 66027

(9) Final report, June 1978

(12) 75 p.

(11) 9 Jun 78

A Master of Military Art and Science thesis presented to the faculty of the U.S. Army Command and General Staff College, Fort Leavenworth, Kansas 66027

dlt

MASTER OF MILITARY ART AND SCIENCE

THESIS APPROVAL PAGE

Name of candidate: Douglas A. Abbott

Title of thesis: Modeled Meteorological Inputs to Environment Dependent Simulation Studies.

Approved by:

John E. Abbott, Research Advisor

Joseph R Bream, Member, Graduate Faculty

_____, Member, Consulting Faculty

Accepted this 1st day of June 1978 by [signature], Director, Master of Military Art and Science.

The opinions and conclusions expressed herein are those of the individual student author and do not necessarily represent the views of either the U.S. Army Command and General Staff College or any other governmental agency. (References to this study should include the foregoing statement.)

ABSTRACT

A stochastic model demonstrates low-cost meteorological support to environment dependent simulation studies. Only the univariate problem is demonstrated, but extentions to multivariate applications are feasible. This application models atmospheric visibility. The model simulates time series at a given geographical point. A historically derived cumulative frequency distribution is converted to its equivalent normal deviate and fitted by a rational approximation. A Markovian time dependence is assumed. Seasonal and diurnal cycles are modeled. A run is initiated via a random draw from a unit normal distribution. Alternately, an initial value may be specified. Subsequent values are generated using a time-correlation weighted linear combination of the prior value and a unit normal random input. This produces a Brownian Movement phenomena within the appropriate probability density function. A given run tends to regress toward the climatological mean while exhibiting random flucuations. A run of sufficient length recreates the probability density functions. Results presented verify model performance against historical data and include a few applications. The FORTRAN computer subroutine is published in an appendix.

ACKNOWLEDGMENTS

Computer resources were provided through the auspices of the Army Command and General Staff College at Fort Leavenworth, Kansas. The author wishes to thank his committee for their many helpful suggestions during the documentation phase of this research. The author is indebted to A. R. Boehm for providing some of the developmental FORTRAN codes used and to both R. M. Miller and A. R. Boehm for numerous enlightening discussions which formed the foundations for the research perspectives presented.

TABLE OF CONTENTS

LIST OF TABLES

LIST OF ILLUSTRATIONS

LIST OF ILLUSTRATIONS - Continued

Figure Page

LIST OF ILLUSTRATIONS - Continued

LIST OF ILLUSTRATIONS - Continued

DEFINITION OF SYMBOLS

AND ACRONYMS

A	A transformation parameter which is a function of t.
AFB	Air Force Base.
B	A transformation parameter which is a function of t.
cfd	Cumulative frequency distribution.
ds	Total differential of s.
END	Equivalent normal deviate, a unit normal function.
FRG	Federal Republic of Germany.
K_i	Density weighted monochromatic absorption coefficient averaged over the near-infrared wavelengths.
K_w	Density weighted monochromatic absorption coefficient averaged over the visible wavelengths.
km	Kilometers.
K_λ	Monochromatic absorption coefficient.
L	Local time on a 24 hour clock.
ln	Naperian logarithm.
m	Meters.
n	A random variable drawn from a unit normal distribution.
p_a	Optical path media density.
pdf	Probability density function.
R	Coefficient of correlation expressing the linear relationship between paired observations lagged in time.

DEFINITION OF SYMBOLS

AND ACRONYMS

A	A transformation parameter which is a function of t.
AFB	Air Force Base.
B	A transformation parameter which is a function of t.
cfd	Cumulative frequency distribution.
ds	Total differential of s.
END	Equivalent normal deviate, a unit normal function.
FRG	Federal Republic of Germany.
K_i	Density weighted monochromatic absorption coefficient averaged over the near-infrared wavelengths.
K_w	Density weighted monochromatic absorption coefficient averaged over the visible wavelengths.
km	Kilometers.
K_λ	Monochromatic absorption coefficient.
L	Local time on a 24 hour clock.
ln	Naperian logarithm.
m	Meters.
n	A random variable drawn from a unit normal distribution.
p_a	Optical path media density.
pdf	Probability density function.
R	Coefficient of correlation expressing the linear relationship between paired observations lagged in time.

DEFINITION OF SYMBOLS AND ACRONYMS - Continued

R_t The value of R when the time lag equals t.

R_1 The value of R when the time lag equals 1 hour.

RMSE Root mean squared error.

RUSWO Revised uniform summary of weather observations.

s Length in meters along an optical path.

T_i Radiation transmissivity averaged over the near-infrared wavelengths.

T_w Radiation transmissivity averaged over the visible wavelengths.

T_λ Radiation monochromatic transmissivity.

TACFIRE The tactical fire direction system, an automated system for control of U.S. Army field artillery assets in support of offensive and defensive military operations.

t Time.

t_0 Subscripted times, e.g., t_0, t_1, ..., refer to specific times.

u Optical path length, as defined by Beer's Law.

v Visibility in meters.

x The END of v.

y x at t plus delta t.

ϵ A transformation constant.

λ Wavelength of electromagnetic radiation.

μ Population mean.

π The radian angle equivalent of 180°.

σ Population standard deviation.

Φ Functional notation.

ϕ Functional notation.

CHAPTER 1

INTRODUCTION

Military decisions are making ever increasing use of decision models. Methods in use range from modeled raw data with human decisions to real world data with modeled decisions. An example of the former is a training simulation and an example of the latter is an aircraft computer flight plan. Within this spectrum, a useful application is weapons performance simulation (e.g., Pickett, et al., 1977). Such simulations provide insight for weapons selection, tactics development, and related applications.

Military decisions tend to be complex. A wide variety of environmental factors are involved. These factors include terrain, seasonal foliage, trafficability, meteorology, electromagnetic environment, and many others. Due to the sheer volume of potential data inputs, some factors receive more emphasis than others. Depending on the application, environmental factors are carefully modeled or ignored. Resource limitations usually preclude consideration of all such dependent variables. Difficult choices are faced in applications ranging from combat operations to laboratory simulations. The goal in each case is to reach a near optimal decision within the time and

resource constraints.

This thesis addresses one subset of the total problem, the meteorological environment. A model designed to provide meteorological support to environment dependent simulation studies is described in Chapter 2. This application is the first operational test of the techniques proposed by Boehm and Abbott (1977). Since the model selected for use is one of several distinct modeling alternatives, a brief rationale is provided to justify the choice. Finally, this chapter outlines the military applications used to demonstrate model capabilities. Results of the demonstrations are presented in Chapter 3. The summary in Chapter 4 provides the author's conclusions, and Chapter 5 offers suggestions for future research.

CHAPTER 2

PROBLEM DESCRIPTION

A self-contained computer subroutine is developed to simulate observed atmospheric visibility. This model is designed to support simulations of broader scope which are dependent upon meteorological conditions. Visibility is selected for demonstration purposes, but any observable atmospheric variable or combination of variables could be substituted.

a. Rationale for Model Choice

There are a number of ways one could build such a model. Options are reviewed in Appendix A. The selected option is the proposal of Boehm and Abbott (1977). There are several reasons for this choice. Clearly, the "no meteorological impact" assumption can be discarded as trivial for the purpose at hand. Newtonian models[1] are prohibitively expensive. They are discussed in Appendix A only because they represent an option and because it is conceivable that they may become a viable alternative in the future. This leaves the historical

---

[1]Models based upon numerical integration of Newtonian physics.

data model[2] and statistical simulation of historical data. The statistical model retains the advantages of the historical data model and overcomes most of the disadvantages. Since the model's attributes have not been fully established, it presents a higher risk; but the potential of the model is worth developing.

b. The Mathematical Model

Details of the mathematical model are presented in Appendix B. A generalized version is available in Boehm and Abbott (1977). A documented computer subroutine is provided in Appendix C.

Conceptually, the model works as follows. The cumulative frequency distribution (cfd) of the event (observed visibility) is estimated from historical data. The cfd is then transformed to an equivalent normal deviate (END) space, and modeled using a rational approximation. Since the probability density function (pdf) is known (the END is by definition a unit normal distribution), a random "walk" through the pdf generates data which can be converted to simulated observations. The time domain is assumed to be a first order Markov process.[3] A "Brownian

---

[2]Models which simply replay recorded observations.

[3]A first order Markov process is a process wherein events prior to the current value have no predictive utility. To the extent prediction is achievable, it is dependent only upon the current value. For a comprehensive guide to the literature, see Whiton (1977).

movement" model is added to produce a tendency for the simulated variable to regress (in time) toward the mean climatological value (the expected value). This generates event frequencies and durations commensurate with observed real-world values.

c. Model Performance

Before proceeding, it is useful to establish that the model produces the desired result. Since the simulation variable is an END, a test of independent, simulated observations amounts to verification that the normal random number generator meets specifications. Having established this, the Markov assumption remains. Boehm and Abbott (1977) tested the model on time sequences of low ceilings occurring at Rickenbacker Air Force Base. Ten years of data were used to estimate the duration of January ceilings below 3000 feet, given a ceiling below 3000 feet at time, 0000L. A simulated climatology was generated from 10,000 model runs. See Figure 1. The Kolmogorov-Smirnov test indicated that the probability that chance could account for the differences between the modeled and estimated distributions exceeded 98%.

A rather important inference can be drawn from this result. It relates to the error introduced by using a rational approximation to model the cfd. Since the curve is smoother, discrepancies will exist whenever the model has fewer degrees of freedom than the number of partitions

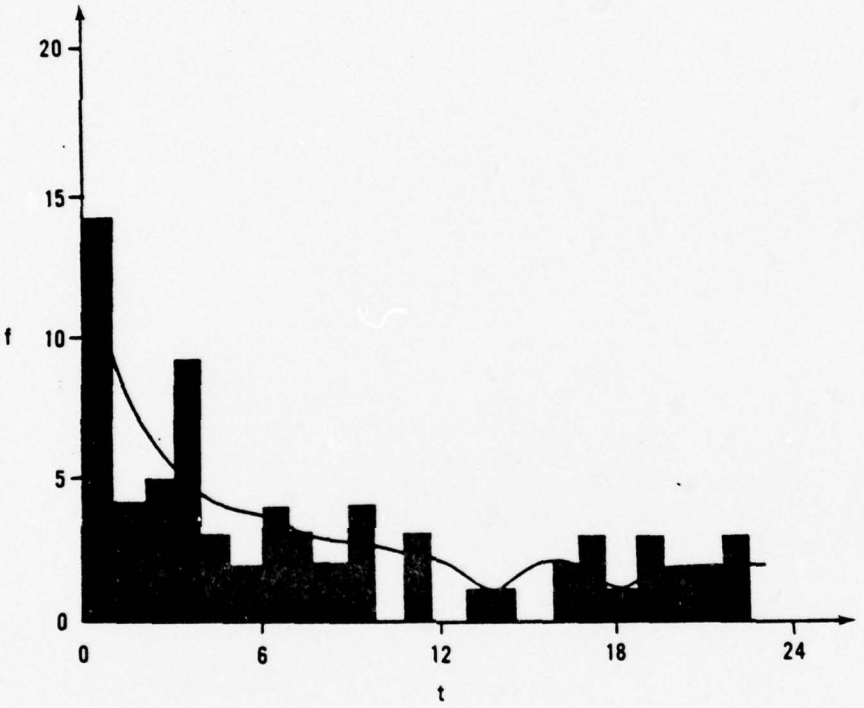

Figure 1. Histogram summarizing 10 years of data for duration of ceilings below 3000 feet. Frequency (f) is plotted against time (t) in hourly increments. There were 94 cases. Duration was truncated at 23 hours and a new series was started. This created a spike at 23 hours. The solid curve is a 10,000 case simulation normalized by frequency for comparison with the 94 real data cases. (After Boehm and Abbott, 1977).

in the estimated distribution. Experience indicates that a root mean squared error (RMSE) less than 10% is acceptable (5% RMSE is more typical). However, in using the model, the Kolmogorov-Smirnov test indicates that the error has not been magnified by the modeling process. A possible explanation for this involves the sampling error in the estimated distribution. The erratic hour to hour variations in Figure 1 are likely to be manifestations of sampling error. It would take over 1,000 years of recorded data to generate a data base comparable to the simulation. Consider now a sample drawn at random from the 10,000 case simulation. See Figure 2. While not a formal proof, visual inspection indicates that the historical sample is at least as representative as the actual population sample. This is formalized by the Kolmogorov-Smirnov results. It is the author's opinion that the simulation may be a better estimate of future probabilities than the historical sample, i.e., the hour to hour variations represent noise in the historically derived distribution.

These results provide some confidence that the model will perform to expectations. Never-the-less, each new application should be verified. A systematic validation of the visibility model is presented in the next chapter.

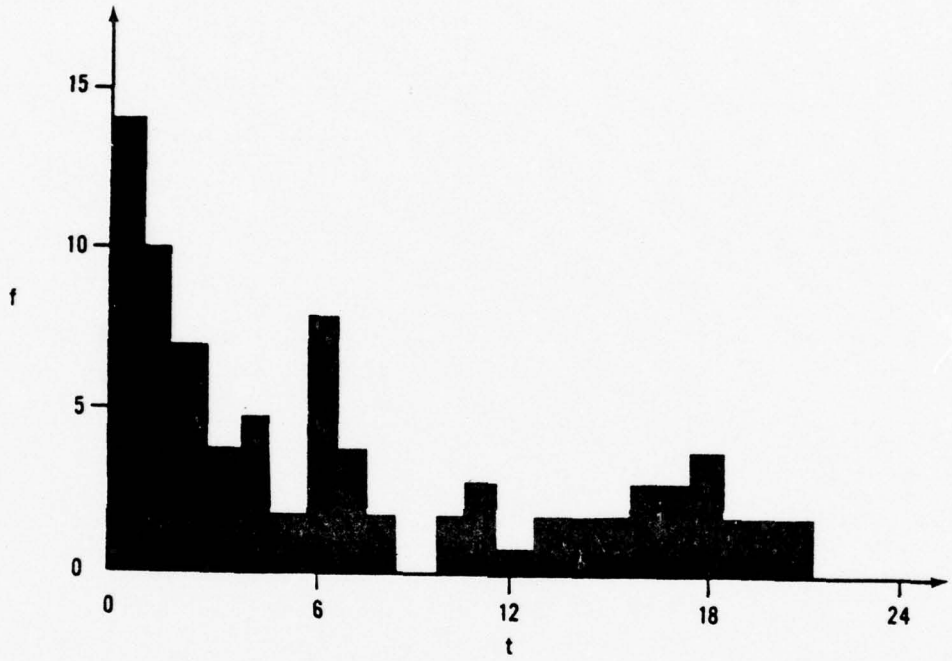

Figure 2. Same as Figure 1, but for 100 cases randomly chosen from the 10,000 case simulation. (After Boehm and Abbott,1977).

CHAPTER 3

RESULTS

Data sources and details associated with deriving the model equations from the historical data cfd are discussed. Next, validity is established by generating a simulated cfd and comparing the simulation to the historical data cfd. Finally, some model applications are presented.

a. Generating the Rational Approximations

The raw data are taken from the United States Environmental Technical Applications Center Revised Uniform Summary of Weather Observations (RUSWO) for Fulda, FRG. The visibility data are distributed into 15 distance intervals; and three, hourly observations are grouped together; see Table 1. For weapon performance simulations, accurate modeling of low visibilities is critical. Therefore, the category thresholds approximating .5, 1, 2, 5, and 7 km are fitted. This insures that the most reliable simulation is obtained for operationally significant values.

The model requires that a specific time be assigned to the cfd vice the three hour composite. Accordingly, the midpoint of the composite period is assumed to be the valid

Table 1. Visibility observations are recorded in units of miles. Reported thresholds are in column 1. The kilometer (km) equivalents are in column 2. Representative thresholds compatible with weapon ranges are .5, 1, 2, 5, and 7 km. The thresholds closest to these values are fitted by regression polynomials. Column 3 lists the transformed thresholds selected for fitting. The column 4 data are from the November, 0000L to 0200L, Fulda, FRG RUSWO. Note that probabilities accumulate upward from 0 miles, i.e., they provide the probability that visibility will be above a given threshold.

v thresholds in miles	Equivalent v in kilometers	Fitted thresholds of $\ln(v + \epsilon)$	Cumulative probability
.00 ≤ v	.0 ≤ v	5.497	1.000
.25 ≤ v	.4 ≤ v		.896
.31 ≤ v	.5 ≤ v	6.616	.896
.50 ≤ v	.8 ≤ v		.862
.75 ≤ v	1.2 ≤ v	7.280	.859
1.00 ≤ v	1.6 ≤ v		.855
1.25 ≤ v	2.0 ≤ v	7.721	.833
1.50 ≤ v	2.4 ≤ v		.810
2.00 ≤ v	3.2 ≤ v	8.150	.792
2.50 ≤ v	4.0 ≤ v		.766
3.00 ≤ v	4.8 ≤ v	8.532	.717
4.00 ≤ v	6.4 ≤ v	8.807	.691
5.00 ≤ v	8.0 ≤ v	9.023	.513
6.00 ≤ v	9.7 ≤ v	9.200	.390
10.00 ≤ v	16.1 ≤ v	10.102	.305

time of the distribution. The diurnal cycle is modeled by eight cfd curves which represent the 24 hour day. This provides three hour interval time resolution. Intermediate values are obtained as required via linear interpolation. Seasonal dependence is provided by using a different set of eight curves for each month. Only the months of September, October, and November are provided in the model. If a month outside this range is requested the model stops execution.

The November raw distribution (i.e., the pdf) for 0100L is shown in Figure 3. November is chosen for display because the higher incidence of adverse visibilities makes the distribution more difficult to fit thereby increasing the errors associated with the fit. The printed value on the line represents event frequency while the intervening values are interval labels. The graph is read as .104 probability that a randomly chosen visibility observation will fall into the 0 to .5 km interval, .037 that it will fall into the .5 to 1.2 km interval, etc. The spike at probability, .305, corresponds to the "good weather" bias. This occurs because interval resolution is lost when visibility exceeds 16.1 km.

Figure 4 provides the cfd corresponding to the pdf in Figure 3. The values are read in the same manner as the pdf except that they accumulate, i.e., the probability of a value below 1.2 km is .104 + .037 = .141, etc.

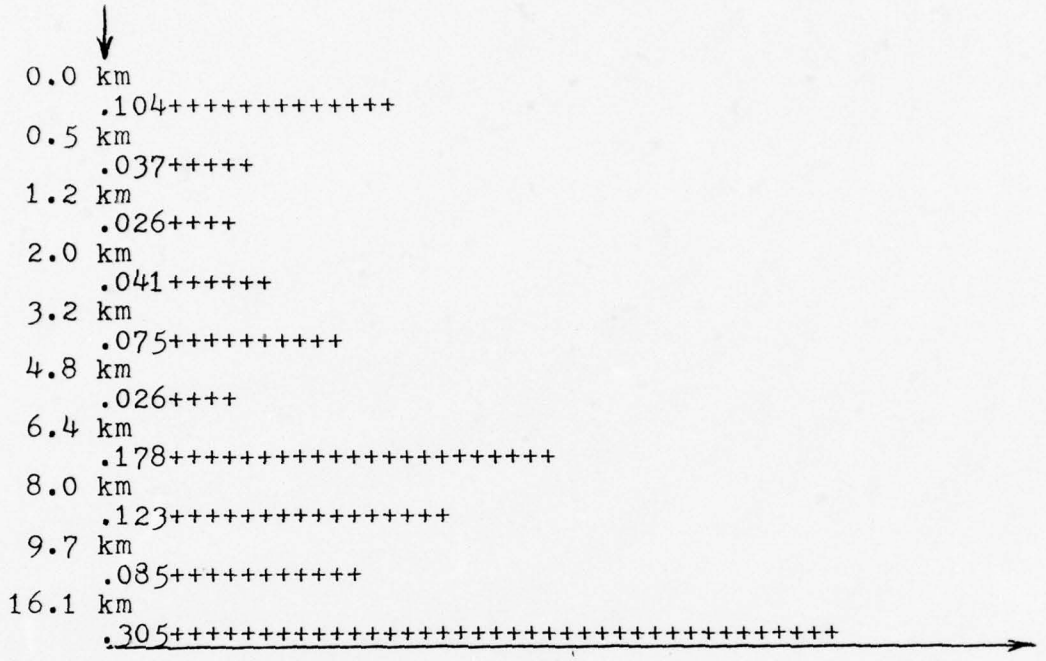

Figure 3. This sample raw distribution (pdf) is generated from Fulda, FRG November RUSWO data, 0000L to 0200L time composite. The values printed at the left of the histogram bar are the probabilities that a randomly chosen observation will fall into the visibility range specified by the numbers immediately above and below the probability; e.g., for the second line, .037 is the probability that a visibility falls within the interval .5 km to 1.2 km.

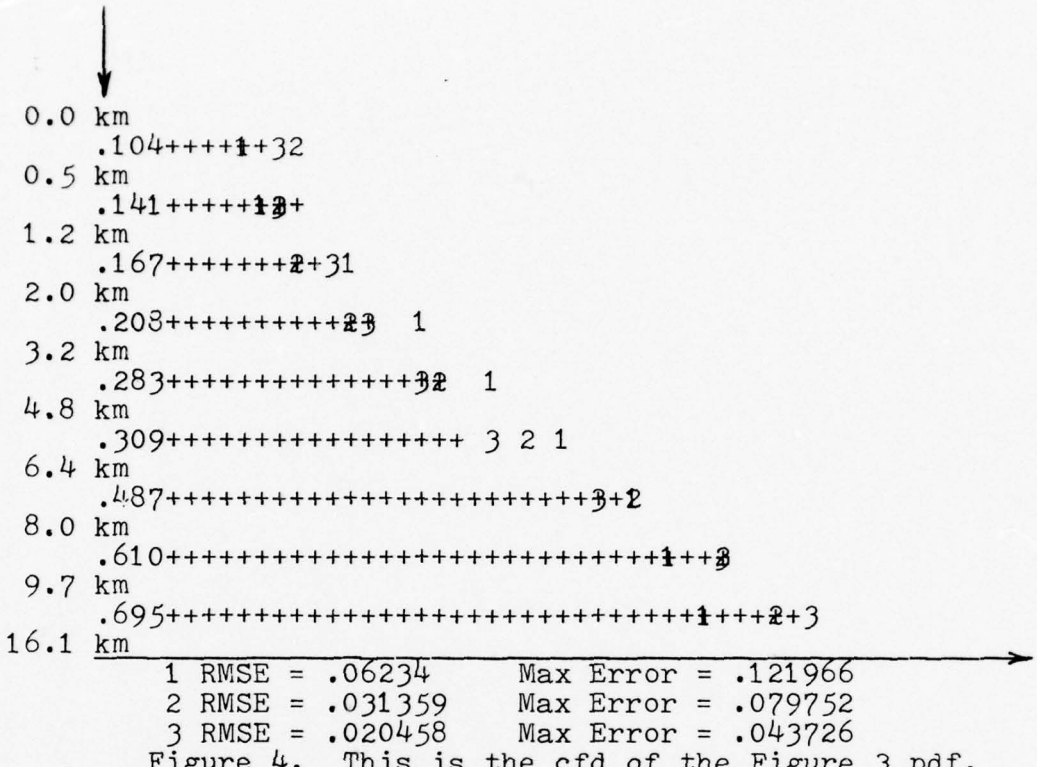

Figure 4. This is the cfd of the Figure 3 pdf. The sums are accumulated upward from zero (the reverse of equivalent values in Table 1). This facilitates military applications. Here the value on the second line corresponds to a probability of .141 (.104 + .037 = .141, using Figure 3 values) that a randomly selected observation will have a value less than 1.2 km. The last bar which brings the ogive to 1.0 has been omitted to facilitate scale expansion in the other categories. The RMSE and maximum error associated with first, second, and third order regression polynomial fits are listed below the cfd. The intersection of these fits, respectively denoted by 1, 2, and 3, is overprinted on the cfd.

The cfd interval thresholds are fitted by a first, second, and third order regression polynomial. The RMSE and maximum error associated with each fit are listed in Figure 4 below the cfd. The first order (linear) fit is selected for use. Based upon analysis of error data, one might be tempted to use a higher order (quadratic or cubic) fit. There is a problem associated with these fits. A region of negative slope exists on each curve. If this region includes realizable values of the simulation variable then one has in effect a region with negative cumulative probability, a serious theoretical deficiency. Boehm (1976) discusses this problem and how to avoid it. In the present case (Figure 4), the quadratic has a usable range from 6.65 to ∞, while the cubic has unlimited usable range. The range of the cubic is adequate, but that of the quadratic is not. However, use of the cubic may generate other problems, e.g., the cubic range may not be adequate for all eight curves in each month and time interpolation may produce problems. Furthermore, some care is required in selecting the proper root when inverting the equation. Finally, there is no guarantee that the higher order fit will produce a more accurate simulation model. When ten class intervals are fitted using two, three, and four free parameters, respectively; it is reasonable to expect a smaller error of fit from the latter two in comparison to the former. However, the higher order fits may be simply capturing the

historical data sampling error. These reasons lead to the linear fit choice. The 12% maximum error in Figure 4 is the largest encountered within the 3 months considered. Linear fit errors are summarized in Table 2.

b. Testing Model Validity

The model is used to generate 5000 independent 24 hour sequences commencing at 0100L. Distributions are created at 6 hour intervals from the 5000 day simulated period of record. The pdf thus derived is shown in Figures 5 through 9. Figure 5 simply verifies the combination of the transformation assumptions and the computer routine which generates unit-normal random numbers. However, this is an important verification since it is the basic building block of the model. Furthermore, a conceivable model application is the simulation of a sequence of independent observations. Figure 5 is precisely this.

Figures 6 through 9 test the Markov assumption through 24 hours. The upper pdf is from the simulation and the lower pdf is from the corresponding historical data. Once more the reasonable agreement between the two is apparent.

The agreement is formally tested using the one-tailed Kolmogorov-Smirnov one-sample statistic. The one-sample statistic is used because the simulation sample is sufficiently large to define a population. This assumption is tested by increasing the number of simulated observations

Table 2. The RMSE and maximum errors produced by a least squares linear regression polynomial fit applied to the historical-data visibility cfd in the transform space. Errors are listed by local time and month.

Time	Sep		Oct		Nov	
	RMSE	Max Error	RMSE	Max Error	RMSE	Max Error
0100L	2.6%	5.9%	3.9%	8.2%	6.7%	12.2%
0400L	3.3%	7.4%	3.6%	7.4%	4.1%	6.9%
0700L	2.7%	4.8%	3.4%	7.2%	3.7%	6.7%
1000L	2.6%	4.5%	3.0%	5.8%	2.8%	4.8%
1300L	1.1%	2.0%	3.2%	7.8%	2.9%	6.0%
1600L	1.2%	3.2%	2.9%	6.8%	3.3%	7.2%
1900L	2.7%	7.1%	2.7%	6.6%	3.6%	6.9%
2200L	3.3%	7.9%	3.3%	7.8%	5.4%	9.2%

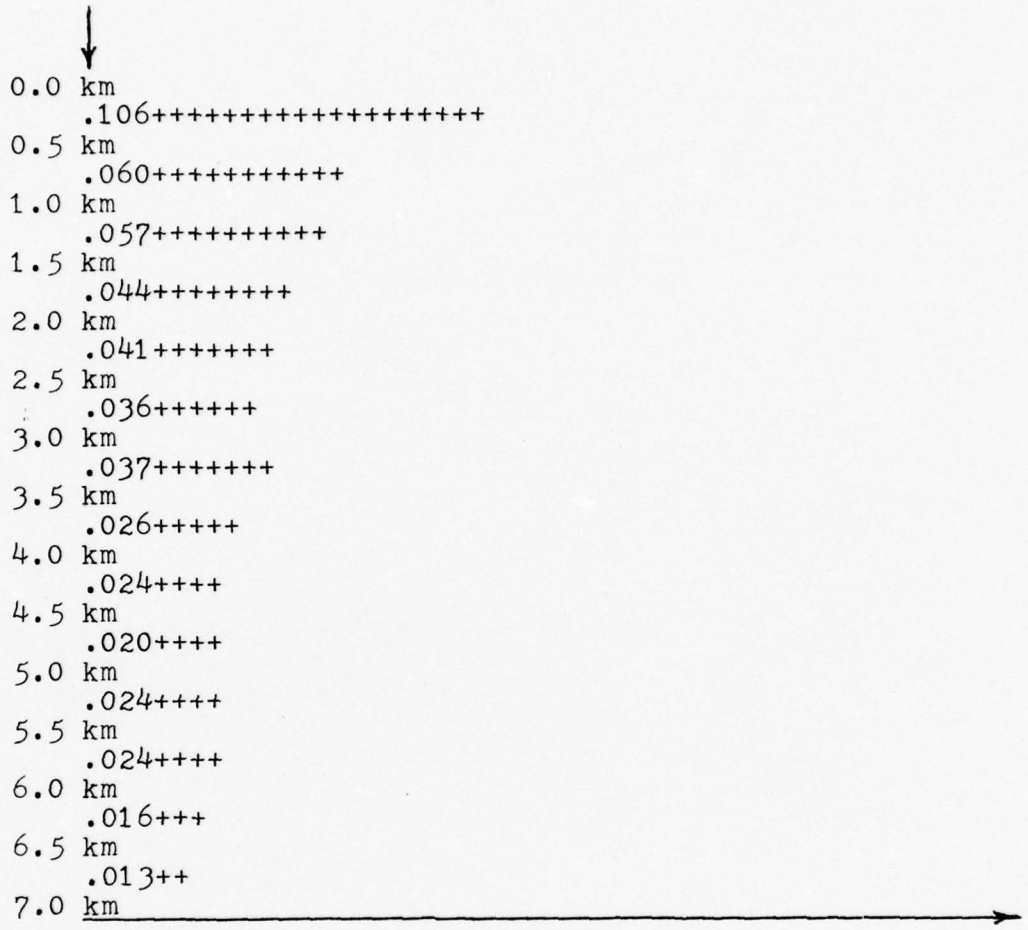

Figure 5. November 0100L simulated pdf for Fulda, FRG. The pdf is a composite of 5000 independent random draws from a unit-normal distribution. Accordingly, this is a test of the random number generator and the linear model, but the Markov time dependence is not tested here. The histogram is read in the same manner as Figure 3, which contains the corresponding time-period historical data. However, the intervals differ.

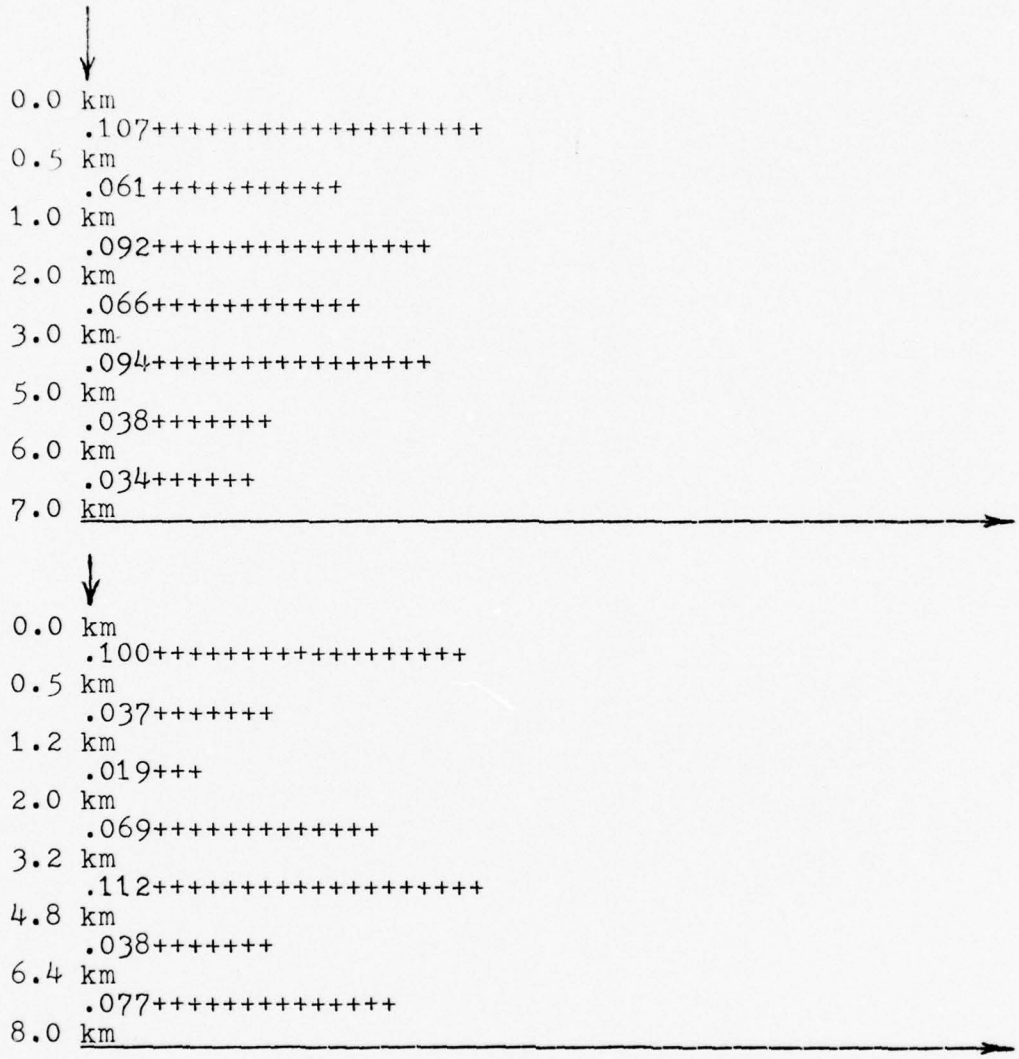

Figure 6. The upper histogram is the pdf from the 5000 day simulation discussed in Figure 5. The data are valid for November 0700L at Fulda, FRG. The data display a composite of the second points in 5000 Markov chains (using a six hour time step) extending from the Figure 5 initial values and employing the linear model of the diurnal cycle. The lower histogram is the historical pdf used to generate the linear simulation coefficients. When comparing values, note that there are minor variations in interval definition. The model provides an excellent approximation, but it is the weakest between the .5 km and 2.0 km thresholds. This is discussed in the text.

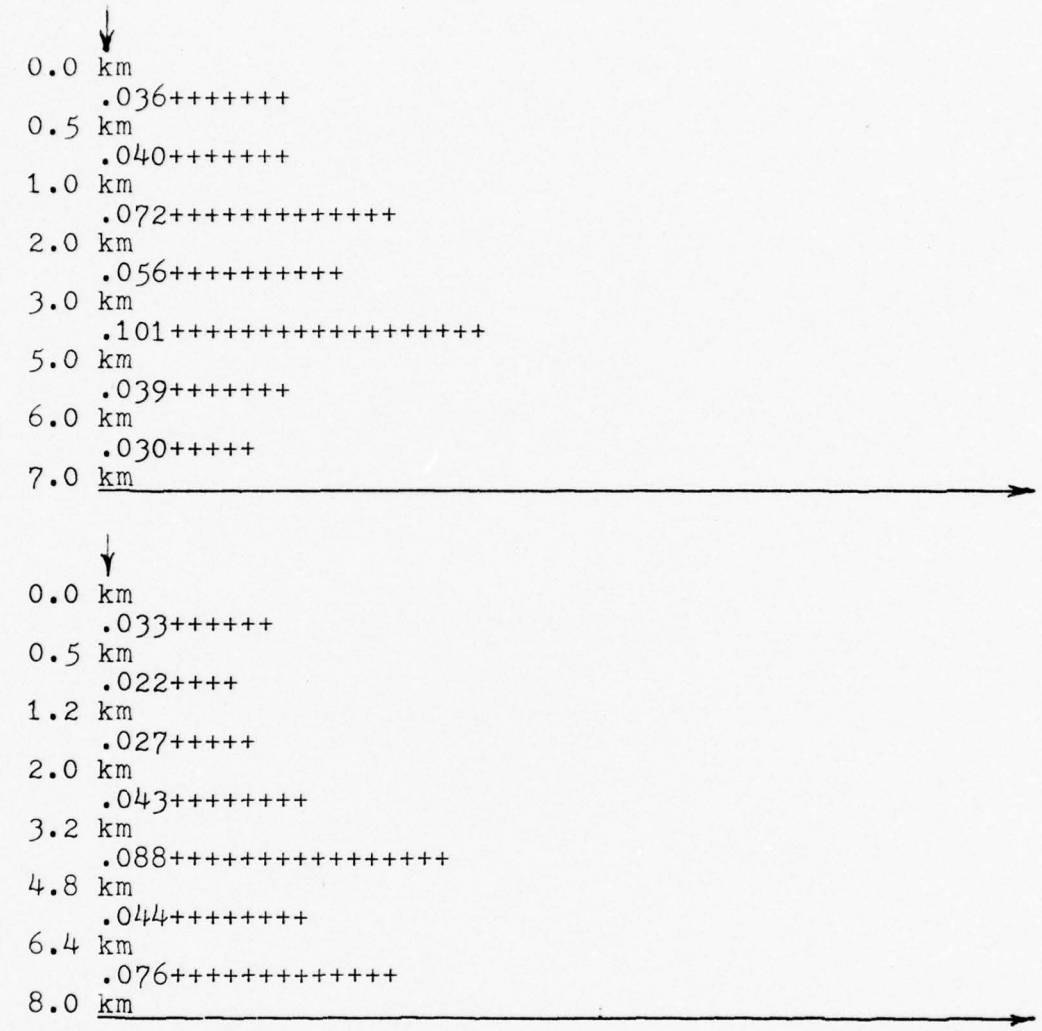

Figure 7. The upper histogram is the pdf from the 5000 day simulation discussed in Figure 5. The data are valid for November 1300L at Fulda, FRG. The data display a composite of the third points in 5000 Markov chains (using a six hour time step) extending from the values associated with Figure 6 and employing the linear model of the diurnal cycle. The lower histogram is the historical pdf used to generate the linear simulation coefficients. When comparing values, note that there are minor variations in interval definition. The model provides an excellent approximation, but it is the weakest between the .5 km and 2.0 km thresholds. This is discussed in the text.

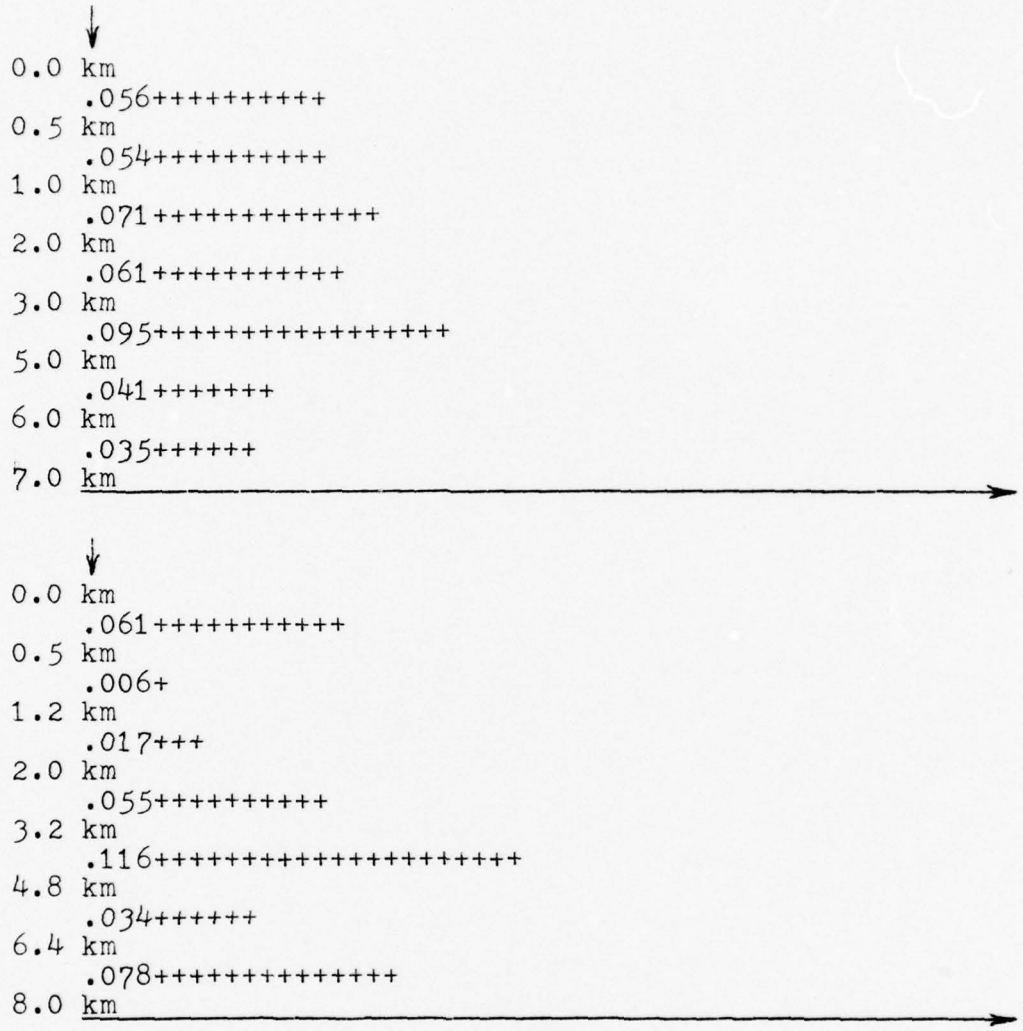

Figure 8. The upper histogram is the pdf from the 5000 day simulation discussed in Figure 5. The data are valid for November 1900L at Fulda, FRG. The data display a composite of the fourth points in 5000 Markov chains (using a six hour time step) extending from the values associated with Figure 7 and employing the linear model of the diurnal cycle. The lower histogram is the historical pdf used to generate the linear simulation coefficients. When comparing values, note that there are minor variations in interval definition. The model provides an excellent approximation, but it is the weakest between the .5 km and 2.0 km thresholds. This is discussed in the text.

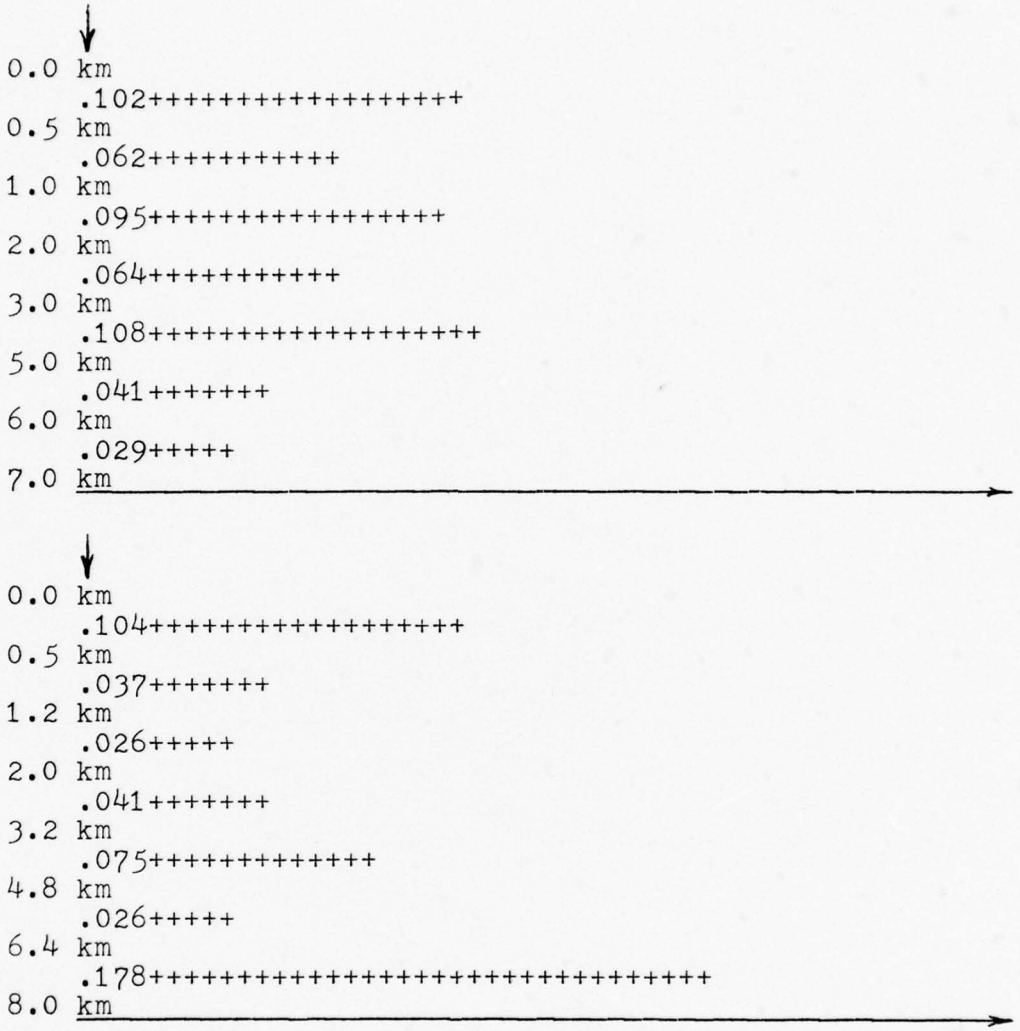

Figure 9. The upper histogram is the pdf from the 5000 day simulation discussed in Figure 5. The data are valid for November 0100L at Fulda, FRG. The data display a composite of the fifth points in 5000 Markov chains (using a six hour time step) extending from the values associated with Figure 8 and employing the linear model of the diurnal cycle. The lower histogram is the historical pdf used to generate the linear simulation coefficients. When comparing values, note that there are minor variations in interval definition. The model provides an excellent approximation, but it is weakest between the .5 km and 2.0 km thresholds. This is discussed in the text.

from 5,000 to 25,000. The distribution does not change within the first three decimal places of event frequency. The one-tailed test is used because the visibility historical distribution tends to be "J" shaped, i.e., bimodal with one mode in the 0 to .5 km interval and the dominant mode in the 16.1 km $\leq$ v interval. Accordingly, a linear model tends to systematically overestimate the cfd between these modes. This tendency is apparent in Figures 6 through 9.

The Kolmogorov-Smirnov statistic tests the null hypothesis that the historical data represent a sample drawn from the simulation population. Assigning large alpha (α = .2) the null hypothesis must be accepted. This equates to a willingness to reject a true hypothesis one in five times. Of course smaller values of alpha are even more restrictive.

c. Model Applications

The application potential has been established by the foregoing verification that modeled data sequences are in reasonable agreement with the data samples observed in nature. It is beyond the scope of this work to seek and verify operational applications. Rather, a contrived example is presented, and it is left to the interested reader to pursue applicability to operational problems.

The demonstration example simulates the probability that an advancing enemy tank will not be visually detected prior to arriving within 3,000 meters of a watchful observer

who has a reasonable field of view. Time commences at 0100L on a typical November day near Fulda, FRG and it runs through 24 hours. Simulation results are displayed in Figure 10. This is a composite of 1,000 trials. The initial visibility is chosen at random from the appropriate pdf. This is a binary event, i.e., visibility above or below 3,000 meters. The 50% probability of visual sighting beyond 3,000 meters is not reached until 0700L. Thereafter, the probability increases rapidly through noon. However, if improvement is not attained by noon, further increase in expectations is markedly reduced.

One might hypothesize that the enemy will advance under cover of adverse visibility conditions. Accordingly, it is assumed that the initial condition is zero visibility (this is a rare event in November; it has probability, 2.5%). Once more a composite is generated from 1,000 cases. Each run is terminated if simulated visibility equals or exceeds 3,000 meters. The simulated expectations are displayed in Figure 11.

The differences produced by the alternative assumptions of $v \leq 3$ km vice $v = 0$ km are apparent in Figure 10 and Figure 11. The probability of v above 3 km increases much more slowly in Figure 11, and the 50% probability is not reached until noon. At the end of 24 hours the probability approximates that associated with the Figure 10, 1300L values. Meteorologically sound arguments can be offered

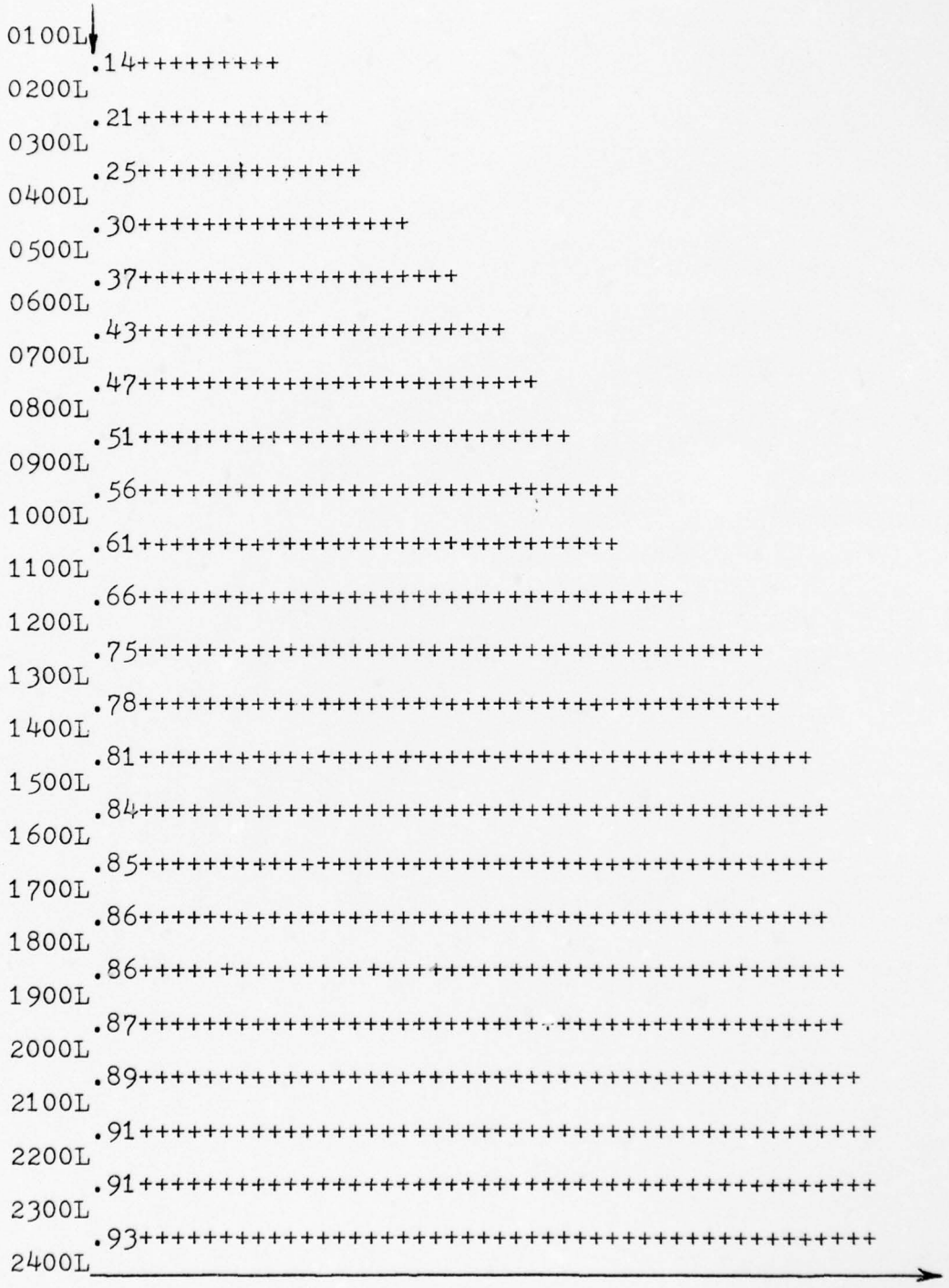

Figure 10. Simulation of the composite time duration (cfd) of 1000 events, v less than 3 km, given that v is below 3 km at 0100L. The 0100L value of v is obtained by repeated random draws from the pdf until the specified criterion is met. 3 km ≤ v terminates a time series.

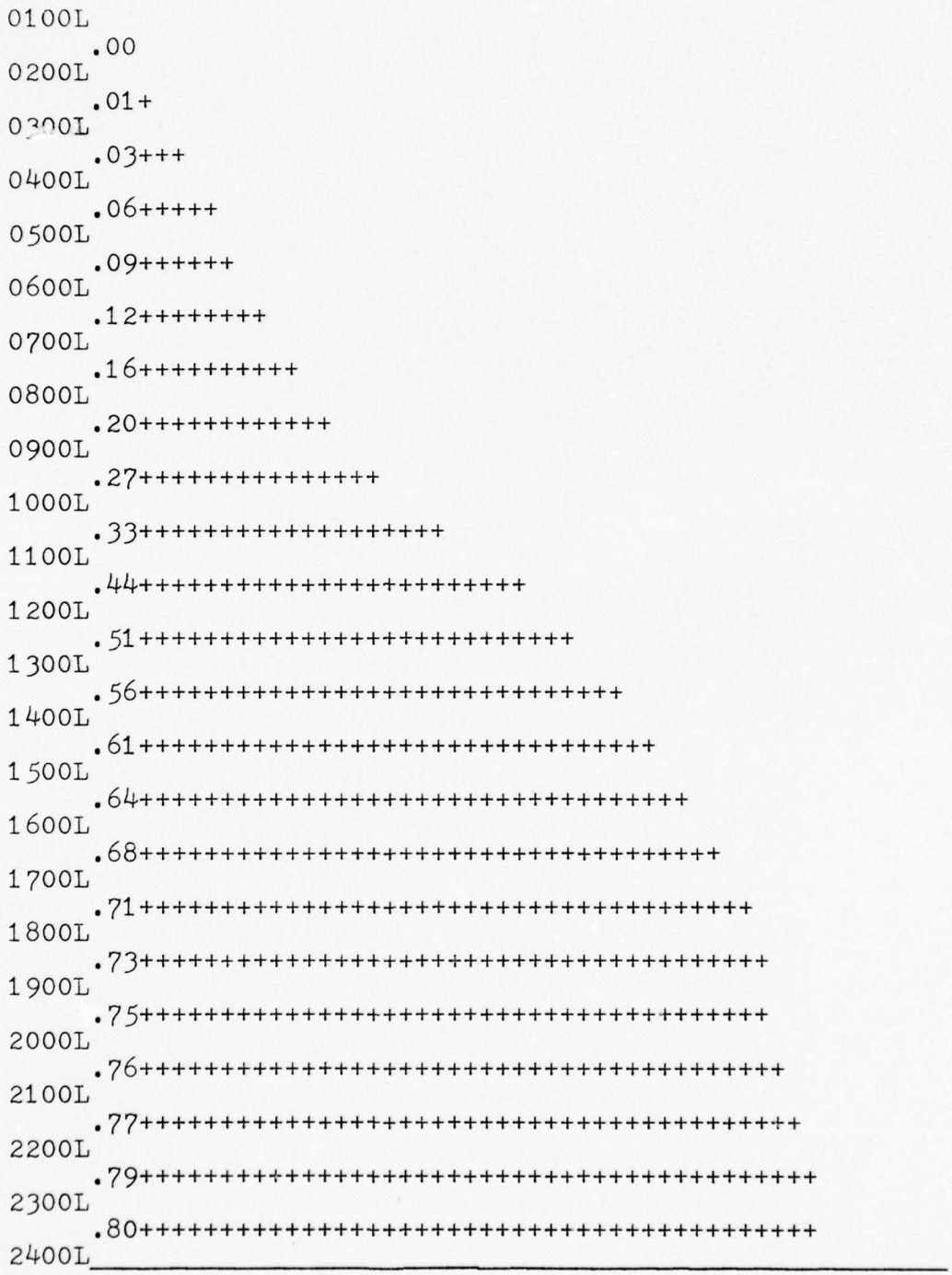

Figure 11. Simulation of the composite time duration (cfd) of 1000 events, v less than 3 km, given that v equals 0 km at 0100L. 3 km ≤ v terminates a time series.

for the differences associated with these related conditional probabilities. Low visibilities are common in morning fog; however, if v = 0 km already at 0100L, the cause is likely to be something other than radiational cooling. One possibility is the synoptic environment associated with recent rainfall and a near stationary front in the vicinity. Such conditions will tend to persist.

Figures 12 and 13 display the tendency for adverse conditions to persist through the morning hours from a different perspective. 1,000 cases are included in each composite. Figure 12 contains simulated distributions at 0300L, 0500L, and 0700L given that the visibility at 0300L equals 1.5 meters. This is a relatively rare event; however, given this condition, probabilities relating to subsequent events can be inferred from the model. Once more the tendency for adverse visibility to persist through early morning, once onset is established, is apparent. Alternately, a random choice (related to historical probability) of visibility below 3 km represents a much more common condition. Again low visibilities persist, but not to the same degree. It should be recognized that a statistical composite such as this contains samples wherein v = 2 km at 0300L goes to 0 km at 0700L as a result of continued radiational cooling, and it contains samples wherein v = 0 km at 0300L goes to 10 km at 0700L with the intervening passage of a frontal system. The former is common and the latter is not, but either is

12(a) 0300L

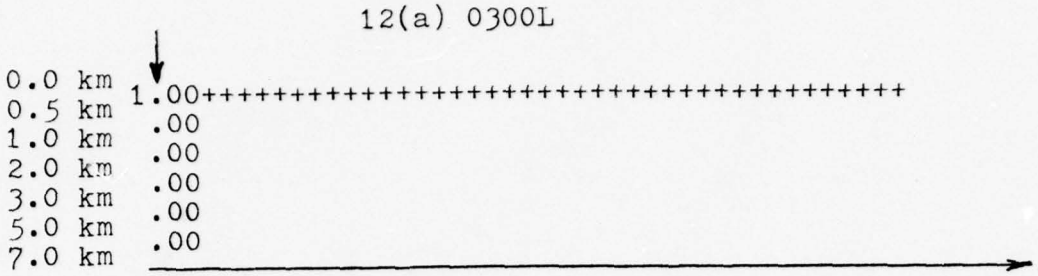

12(b) 0500L

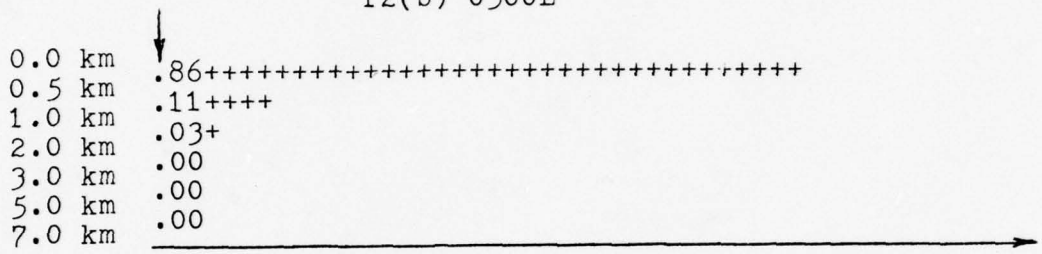

12(c) 0700L

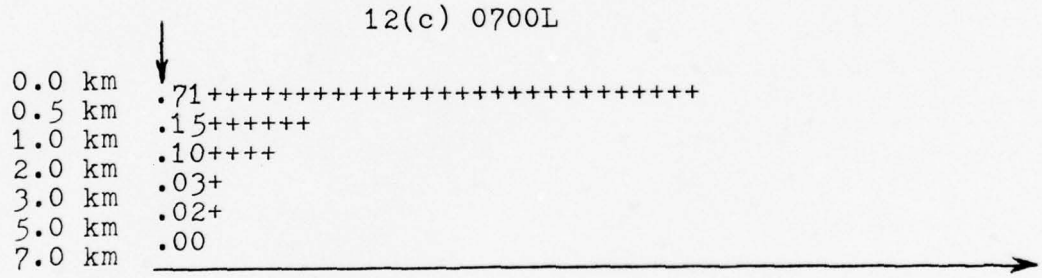

Figure 12. Rare event climatology is generated via simulation. In 12(a), v is assigned the value, 1.5 m, at 0300L. One thousand trials are composited. 12(b) displays the resulting conditional pdf at 0500L, and 12(c) displays the conditional pdf at 0700L. Meteorological insight into these events and their time evolution is offered in the text.

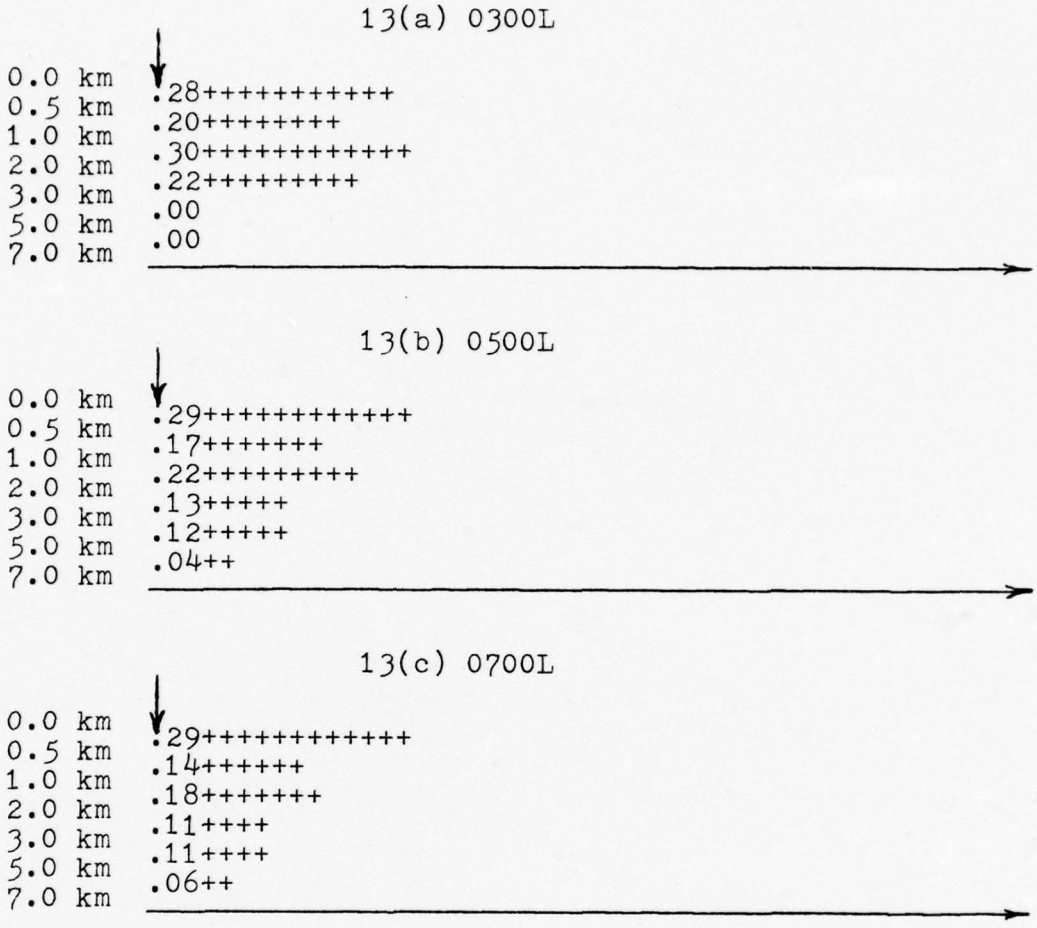

Figure 13. Conditional climatology is generated via simulation for comparison with Figure 12 rare event conditional climatology. One thousand trials are composited. In 13(a), v is selected randomly from the portion of the pdf containing the event, v less than 3 km at 0300L. 13(b) displays the resulting conditional pdf at 0500L, and 13(c) displays the conditional pdf at 0700L.

realizable within a particular simulation set. The relative probabilities are brought into perspective only by a large composite of simulations.

The model capabilities have now been demonstrated. Figure 5 illustrates a composite sequence of independent observations. Figures 6 through 10 provide applications from simulated serial observations. Finally, Figures 11 through 13 demonstrate the capability to rerun a vignette with altered assumptions.

The capabilities of the model are apparent, but it is equally apparent that one would like additional options. The example just presented assumes that the enemy observes and reacts to current events but lacks predictive skill and the ability to alter the visibility environment. A more realistic requirement might be for an initial visibility of zero meters plus at least an 85% expectation that visibility will remain below 2,000 meters for a minimum of five hours. This allows some time for the enemy to react once these conditions are met. Finally, the enemy may choose to employ artillery smoke if visibility exceeds 1500 meters following initiation of his movement. Simulation of meteorological aspects of this relatively more complex vignette is beyond the capability of the simple model presented here, but it is not beyond the capability of the generalized methodology. Problems with complexity equal to or greater than this provide the requirements which will

ultimately unite resources with knowledgable researchers and produce a generalized simulation capability.

CHAPTER 4

SUMMARY AND CONCLUSIONS

A first order Markov model is used to simulate atmospheric visibility observations. In its present form, the suggested use of such a model is to support environment dependent simulation studies. The model is inexpensive to operate and self-contained. It is capable of generating sequences of either independent or serially correlated observations. The initial value of a correlated sequence may be specified or obtained via a random draw from the pdf. No control is exercised over subsequent values; they are a function of the previous value in the series, the serial (time) correlation, and an imposed random variation.

The model generates visibilities valid at a geographical point, Fulda, FRG. However, the methodology is more general. Visibilities at any geographical point can be simulated if appropriate values of the model parameters, A and B, are introduced. The correlation, R_1, is reasonably robust. A geographical shift does not normally require a change.[1] Furthermore, any single meteorological

---

[1] Boehm, personal communication.

variable can be modeled using this general approach; however, instead of simply changing model parameters, an alternate mathematical expression (rational approximation) for the END is needed if the variable is not log-normal. Simultaneous modeling of several variables at multiple locations is also feasible. This more difficult problem is discussed in the next chapter.

Typically, environment dependent simulation studies model meteorological dependence by rerunning historical sequences. The stochastic model demonstrated here is capable of providing this support and more. The simulation model duplicates the positive features of the historical model and it does not suffer from the negative features. Advantages afforded by the stochastic model are:

- Minimal computer assets are required. The univariate meteorological simulation lies within the capabilities of a hand-held programmable calculator.

- Simulation is not limited by the finite sequences available in recorded history.

- Cumbersome file manipulation associated with the historical model is avoided.

- Vignettes dependent upon a given initial value of the meteorological variable are easily supported. Historical models require cumbersome record searches; and for rare events, recorded data may be inadequate.

- Sensitivity analyses are easily supported

by the simulation model.

- If a sequence of independent values is required, the serial correlation inherent in historical data is easily avoided.

The focus has been upon simulation support. The methodology has operational utility as well. For example, if the initial value of a sequence is the current observation, a forecast can be generated in time or space.[2]

Forecasting in time is common, but less is known about how to successfully forecast in space. However, if these capabilities are demonstrated, a number of applications result. An example is optimal placement of meteorological observations in time and space to support field artillery operations. Another is preselection of prepared weapon positions as a function of the small scale variations in climatology. These climatic variations can be modeled when available data are inadequate to provide a historical data estimate, e.g., remote regions or enemy territory. The list of potential uses is extensive, but research is required if these capabilities are to be realized.

---

[2]The mathematical formulation differs somewhat. See Tahnk (1975) and Boehm (1976).

CHAPTER 5

SUGGESTIONS FOR FURTHER RESEARCH

Modeling the time evolution of a multivariate distribution must be demonstrated if the final enclave of historical data model applications is to be breached by simulation. Precise time-space predictions at any specified resolution are a required capability which is not available today. Promising methods have been proposed; however, difficulties will undoubtedly be encountered during the applied research phase of model development.

An important theoretical question in meteorology is the definition of optimal time and space positioning within the global or regional observational networks. This is an economic problem. The requirement is to determine the point at which the cost of the observations exceeds the benefits to be derived from the data applications. On a smaller scale, the United States Army faces precisely the same problem. The optimal time-space resolution of observations taken in support of field artillery operations is unknown. The simulation technique presented here, together with the capability extensions which appear to be feasible, can address such questions. For example with the new TACFIRE system providing a significant computer capability within each

artillery battalion, a network of meteorological observations can be adjusted in space and time via simulation to coincide with the position of each artillery tube. Corrected observations can be generated in seconds. Thus, relocation of the tubes does not degrade environmental support. The system would require input of a few numbers following each meteorological observation. Currently, meteorological parameters are often assumed constant between successive time observations and they are linearly interpolated or extrapolated in space. Research is needed to provide the economic limitations of increased sophistication. The benefits appear to be significant. Small improvements in the accuracy of an artillery delivered mine field have a potentially high wartime utility.

The technological sophistication of the battlefield is constantly increasing. The small number of environment dependent applications represents the tip of an iceberg of potential current and future applications for a stochastic meteorological simulation model taken in conjunction with existing microprocessor technology. In many situations, operational applications still use World War II methods to exploit environmental data. Research is needed to determine what is possible and produce corresponding capabilities. The high price tag associated with sophisticated weapons limits the acquisition rates. Technology of the type proposed herein can in principle increase utility and

effectiveness of such systems thereby offsetting acquisition limitations.

It is not intended to imply that the method presented is the only feasible approach. Many components of the problem are being pursued by Air Force Geophysics Laboratory at the request of the Air Weather Service. Several alternative methodologies are being explored. It is the author's opinion that current efforts are small in relation to the large potential benefits which are obtainable.

APPENDIX A

APPENDIX A

METEOROLOGICAL MODELS

The meteorological models available for simulation applications cover a wide range of complexity and cost. On one end of the spectrum is the "no meteorological impact" assumption. It is simple, but the cost is low only if the assumption is correct. The other end of the spectrum reaches into the fringe areas of applied, if not basic, research.

The model used in this study is a statistical simulation of historical data proposed by Boehm and Abbott (1977). This and alternative modeling options are reviewed.

a. The No Impact Assumption

One can easily conceive a scenario which is not dependent upon meteorological variables. A simple example is a battle simulation which is initiated and concluded within a matter of minutes. Here the assumption is not "no impact;" it is "no time variation" since initial conditions are not expected to change during the course of the simulation. Accordingly, a mean value (or a best/worst case value) can be assigned and held constant for the simulation.

In the example just presented, formal testing is

not used in choosing to freeze meteorological conditions in time and space. The choice is a personal judgement (e.g., a personal probability; Savage, 1954). Such judgments are powerful tools when based upon expert opinion. Alternately, one could formally test a no impact hypothesis (Spiegel, 1975). When only one variable is being considered, it may be simpler to model the variable than to establish that modeling is unnecessary. On the other hand, testing may be valuable if one wishes to show that modeling a univariate dependence is adequate, i.e., a multivariate treatment is unnecessary. Multivariate models are considerably more complex than their univariate counterparts. Research is needed to improve multivariate modeling.

b. Modeling Meteorological Impact

Models of the meteorological environment fall into three general categories; historical data models, Newtonian models, and stochastic models. References in each category are included to illustrate the general approach in current use rather than to provide a developmental audit trail.

(1) Historical Data Modeling

A historical data model uses time-sequenced data to provide meteorological inputs to a simulation model. Spatial variation can be added, but this presents an interpolation problem because recorded observations are spatially sparse (they may be located tens of kilometers apart in densely populated industrial societies or thousands of

kilometers apart over the oceans of the Southern Hemisphere).

This model has both good and bad features. On the positive side, it is inexpensive (given adequate mass storage handling capability); a reasonable time sequence of events is maintained (e.g., a realistic time lag is guaranteed for a clear sky to become overcast); and joint occurrence probabilities for multivariate applications are reasonable (e.g., rain does not fall from a cloudless sky). The latter two features are obvious since the model is nothing more than a replay of recorded history. On the negative side, it is difficult to estimate the sampling error and for some applications, the data are perishable.

Consider perishability. An example is a sensitivity analysis. If meteorological inputs are held constant while other parameters are varied, one risks tuning a decision to a historical meteorological sequence. This situation is not unlike a statistician always entering his random number table at the same point during a sequence of related experiments. Random variations of weather inputs would seem preferable even though subsequent analysis may be made more difficult.

In summary, historical data models are inexpensive and easy to use. Given a short suspense, they may offer the only option; however, some care should be exercised when interpreting results from sequential use and reuse

of limited data.

(2) Newtonian Models

Newtonian models are used extensively in generating operational forecasts of meteorological conditions (Shuman and Hovermale, 1968). They are also used to simulate global climate (Manabe, 1969). These models require numerical solution of physical laws (expressed mathematically). Newton's laws of motion, mass-energy conservation, and thermodynamic laws are cast into a set of nonseparable partial differential equations. These equations can be solved approximately if a number of simplifying assumptions are made. Currently, only deterministic models are in operational use; however, in principle, it is possible to estimate the time/space evolution of the initial uncertainty (Fleming, 1970).

Newtonian models have not been used to generate meteorological input variables for problems of the type being considered here. There are two obvious reasons. The first is cost. These models can dominate a large computer. The second is that model outputs do not directly provide values of the dependent variables normally needed. Statistical methods can be used to convert outputs into the needed variables (Klein and Glahn, 1974); however, it then becomes cost-effective to use a statistical method directly.

(3) Stochastic Models

Stochastic forecast models have been used to generate meteorological forecasts for over ten years. These models (used either directly or in combination with Newtonian models) are promising to automate many forecasting tasks currently being performed manually. The most common approaches employ discriminant analysis (Miller, 1962), equivalent Markov regression (Miller, 1964), nonlinear regression (Miller, 1969), or Markov chains (Gringorten, 1966 and Boehm, 1976). Boehm and Abbott (1977) use a Markov process to generate equivalent historical data. The methods extends earlier work by Gringorten (1966) and McCabe (1968).

The stochastic models all operate on the same general principles. Historical data are used to estimate the correlation between present and future events. These relationships are then used to generate a time series. Methods for spreading the time series in space have been proposed by Von Luetzow (1973) and Gringorten (1976). The model outputs are probabilistic by nature, but one can easily devise rules for converting to deterministic values if they are needed.

APPENDIX B

APPENDIX B

MODEL DESCRIPTION

Simulated historical data are generated by a computer to provide representative values of atmospheric surface visibility. Representative values means that event frequencies and durations correspond to those found in the observed climatological distribution. Of course, deviations the order of magnitude of observed year to year variability are both acceptable and desirable. The model used is that proposed by Boehm and Abbott (1977). It is adapted to the one variable under consideration. The visibility climatology of any geographical point could be simulated by this model if the distribution equations are known and introduced into the computer program.

a. Modeling Surface Visibility

The model employs normal time series theory. Accordingly, raw values of visibility must be generated from the END. Visibility is known to be log-normal (Chisholm and Kruse, 1974). This means that the transformation:

$$x = A \ln(v+\epsilon) + B \qquad (1)$$

produces a normal variable, x, where v is visibility in meters (nondimensionalized). The constant, ϵ, is needed to avoid the rapid slope change and singularity as v approaches

zero.[1] The coefficients, A and B, are given by:

$$A = \sigma^{-1} \tag{2}$$

and

$$B = -\mu\sigma^{-1} \tag{3}$$

where μ is the mean and σ is the standard deviation of the ln v population, i.e., x is the standard normal of ln v.[2] A and B are functions of time.[3] This is where the diurnal and seasonal cycles are taken into account within the model. Diurnal variations are modeled by defining the distribution coefficients at equal intervals over a 24 hour period, and seasonal variation is modeled by developing distinct coefficients for each month.[4] Intermediate diurnal distributions are obtained as needed via linear interpolation for diurnal cycles. The impact of the transformation is seen schematically in Figure 14. Generating the END is an approximate and highly nonlinear process as compared to the linear transformation associated with variable standardization. The latter produces a unit-normal if and only if

---

[1] $\epsilon = 244.$ is selected by trial and error.

[2] This simple relationship of v to x is the result of á priori knowledge of the distribution. Boehm (1976) provides guidance for deriving the END when the distribution is unknown.

[3] Historical meteorological data are used to estimate A and B.

[4] Alternately, one could represent the annual variation as either two seasons (warm and cold) or four seasons.

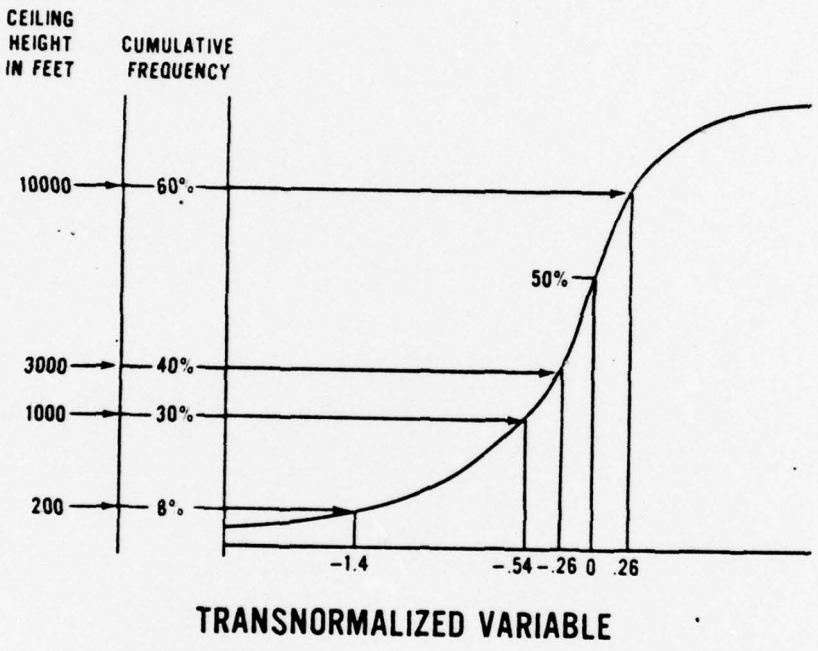

Figure 14. The transformation of cumulative frequency of ceiling height to its END is depicted schematically. The allowable END variable range is from minus to plus infinity. (After Boehm and Abbott, 1977.)

the original distribution is normal.

Analytic expressions are now available for the pdf and cfd. Using functional notation, let $\phi(x)$ = pdf, and let Φ = cfd. Then by definition:

$$\phi(x) = (2\pi)^{-\frac{1}{2}}\exp(-\tfrac{1}{2}x^2) \qquad (4)$$

and

$$\Phi(x) = \int_{-\infty}^{x}\phi(w)dw \qquad (5)$$

where w is a dummy variable.

Applications dictate model use at this point. Assume that a weapon's performance is dependent upon the instantaneous value of visibility. The model simulates a value of x using a normal random number generator, and (1) can be solved for v since A and B are known parameters.

A more interesting problem is a decision simulation which is dependent upon current visibility and subsequent values at the same location, but over a specified time interval, e.g., 12 hours. In this case, the simulation must address the correlation between successive values of visibility in the time domain. Given x, the END of visibility at time, t_o, let y equal the END at a subsequent time, t_1; and let R equal the correlation between x and y. Since x and y are both normal, the joint distribution of x and y will be given by:

$$\phi(x,y) = [2\pi(1-R^2)^{\frac{1}{2}}]^{-1}\exp[-\tfrac{1}{2}(x^2+Rxy+y^2)/(1-R^2)] \qquad (6)$$

A relationship which will produce the result in (6) is:

$$y = Rx + (1-R^2)^{\frac{1}{2}}n \qquad (7)$$

where n is a unit-normal random variable (Feller, 1966).

Recursive use of (7) from t_0 to t_1, t_2, ... defines a simulation algorithm. Since y at each step is related to x of the preceding step via the parameter, R, (7) produces a first order Markov process if $R_t = R_1^t$. R_t is the value of R at time, t; and R_1 is the value of R at t = 1 hour.[5] Weather events such as visibility are well approximated by a first order Markov process (Tahnk, 1975). The simulation algorithm, (7), will tend to regress toward the mean value (Feller, 1966), but the random input will produce a fluctuation about the mean.

b. Converting Visibility to Transmissivity

Some applications require atmospheric transmissivity rather than visibility. Accordingly, it is useful to derive a relationship which converts simulated visibility into transmissivity. Beer's Law states:

$$T_\lambda = \exp(-k_\lambda u) \tag{8}$$

relating the monochromatic transmissivity, T_λ, to the optical path length, u, via an absorption coefficient, k_λ (Fleagle and Businger, 1963). T_λ is defined as the ratio of incident to transmitted radiation at wavelength, λ; and the optical path is defined as:

---

[5] R_1 is estimated from historical data. Use of this continuous exponential definition of the time decay of R actually defines an Ornstein-Uhlenbeck process, the continuous counterpart of a first order Markov process.

$$u = \int_o^s p_a ds \tag{9}$$

where p_a is path media density and s is path length. For small intervals of λ, k_λ may be assumed constant; and for small s, horizontal gradients of p_a may be neglected near the earth's surface. Substituting v for s, Beer's Law can be written:

$$T_w = \exp(-K_w v) \tag{10}$$

T_w is mean transmissivity over the visible spectrum range, $.4 \leq \lambda \leq .7$ microns,[6] and K_w is a density weighted absorption coefficient. The near infrared spectrum, $7 \leq \lambda \leq 11$ microns, is also of interest. Using the prior assumptions with analogous notation gives:

$$T_i = \exp(-K_i v) \tag{11}$$

The empirical relationship, $K_i = .83K_w$, provides an estimate of K_i. With the parameters thus defined, (10) and (11) provide the needed relationships for deriving transmissivities from simulated visibilities.

A word of caution is in order. Beer's Law is strictly valid only for monochromatic transmissivity with negligible scattering and emissivity at the wavelength under consideration. The above relationships are crude (particularly for the near infrared) and should be used with discretion. See Craig (1965) for a detailed discussion.

---

[6] One micron equals 10^{-6} meter.

APPENDIX C

APPENDIX C

MODEL SUBROUTINES

IN FORTRAN

The FORTRAN function PAWSES returns a simulated visibility, $0 \leq v \leq 30$ km. PAWSES has three arguments, DELT, RKIND, and MNTH, which must be supplied by the user. Rules for applying the function are provided within the code. The remainder of the functions which are accessed by PAWSES are transparent to the user. However, the system subroutines and functions must be supplied if not available in the library. These are listed with a brief description of their purpose. Examples which demonstrate all user options are provided.

a. The FORTRAN Code

```
      FUNCTION PAWSES (DELT,RKIND,MNTH)
C  PROTOTYPE AWS ENVIRONMENT SIMULATION (PAWSES) FUNCTION:
C  11 MAY 78 VERSION BY ABBOTT.  PAWSES RETURNS A SIMULATED
C  VISIBILITY, 0.LT.V.LT.30 KM, IN A RANDOM SEQUENCE WHICH
C  SIMULATES ACTUAL WEATHER.
C
C  THE USER MUST SUPPLY 3 ARGUMENTS.
C
C    1.  DELT:  A NEGATIVE DELT GENERATES AN INITIAL
C        VALUE,V(1), OF A NEW SEQUENCE VALID AT TOD=-DELT
C        WHERE TOD IS TIME OF DAY IN HOURS.  TO GENERATE
C        N ADDITIONAL VALUES; V(2), V(3), ..., V(N); DELT
C        IS THE POSITIVE TIME INCREMENT IN HOURS BETWEEN
C        V(1) AND V(2), V(3) AND V(4), ETC.  THE SUCCESSIVE
C        V(I) NEED NOT BE EQUALLY SPACED IN TIME.
C
C    2.  RKIND IS REFERENCED ONLY WHEN DELT IS NEGATIVE.
C        IT CONTROLS THE TYPE OF SEQUENCE TO BE GENERATED.
```

```
C       THERE ARE 3 OPTIONS:
C            A.  IF(ABS(RKIND).GT.30.) THE RANDOM NUMBER
C       GENERATOR SEED IS RESET TO THE VALUE RKIND.
C            B.  IF(15..LT.ABS(RKIND).AND.ABS(RKIND).LT.30.)
C       END = RKIND + 20. OR RKIND - 20. RESPECTIVELY FOR
C       NEGATIVE AND POSITIVE VALUES OF RKIND.
C            C.  REMAINING VALUES OF RKIND SELECT THE END
C       RANDOMLY FROM THE VALUE RANGE -3.3 TO 3.3.
C
C     3.  MNTH SPECIFIES THE MONTH FOR WHICH A REPRESENTA-
C       TIVE SEQUENCE IS DESIRED.  THIS VERSION HAS ONLY 3
C       MONTHS, SEP, OCT, AND NOV.  IF MNTH DOES NOT HAVE
C       THE VALUE 9, 10, OR 11, EXECUTION IS STOPPED.
C
      DATA X,ISEED,OLD/0.,0,1.E10/
      IF(MNTH.GT.11) GO TO 20
      IF(MNTH.LT. 9) GO TO 20
      IF(DELT.GT.0.) GO TO 50
      IF(ABS(RKIND).LT.30.) GO TO 10
      ISEED = 1
      X = RKIND
      CALL RANSET(X)
      GO TO 1
   10 IF(ABS(RKIND).LT.15) GO TO 1
      E = RKIND + 20.
      IF(RKIND.GT.0.) E = RKIND - 20.
      TOD = -DELT
      GO TO 3
   50 IF(DELT.EQ.OLD) GO TO 2
C
C  THIS SECTION FOR CHANGE IN DELT
C
      R =.95**DELT
C  R IS CORRELATION FROM ONE TIME TO TIME PLUS DELT
      D = SQRT(1.-R**2)
      OLD = DELT
      GO TO 2
C
C  THIS SECTION FOR NEGATIVE DELT.  IT GIVES NEW TOD.
C
    1 TOD = -DELT
      E = RANDOM(X,ISEED)
      GO TO 3
C
C  THIS SECTION FOR POSITIVE DELT.
C
    2 E = R*E + D*RANDOM(X,ISEED)
      TOD = AMOD(TOD+DELT,24.)
      IF(E.GT.3.3) E = 3.3
      IF(E.LT.-3.3) E = -3.3
    3 PAWSES = XRAW(E,MNTH,TOD)
```

```
      RETURN
   20 STOP1
      END


      FUNCTION RANDOM (X,ISEED)
      IF(ISEED.GT.0) GO TO 2
      ISEED = 1
      CALL SECOND (X)
      CALL RANSET (X)
    2 S = 0.
      DO 4 I=1,12
      X = RANF (X)
    4 S = S + X
      S = S - 6.
      RANDOM = S
      RETURN
      END


      FUNCTION XRAW (E,MONTH,TOD)
      DIMENSION A(2),B(2),COEF(2,8,12)
      DATA COEF/128*0.,-3.7737,.35767,-2.5142,.28516,
     1  -2.6612,.32512,-4.6655,.50725,-10.391,1.05796,
     2  -8.7369,.82468,-6.0119,.53009,-5.22585,.4519,
     3  -3.2424,.3006,-2.7119,.30975,-2.6765,.3194,
     4  -3.90145,.43904,-6.6982,.6888,-7.5218,.7588,
     5  -6.731,.67966,-4.1589,.359,-5.1006,.5774,
     6  -5.2522,.60202,-4.9336,.55584,-50687,.5636,
     7  -5.9769,.63807,-5.6332,.59148,-5.6805,.61517,
     8  -5.273,.5885,16*0./
      IT = TOD + .01
      J = (IT-1)/3. + 1
      A(1) = COEF(1,J,MONTH)
      A(2) = COEF(2,J,MONTH)
      JJ = J + 1
      IF(JJ.EQ.9) JJ = 1
      B(1) = COEF(1,JJ,MONTH)
      B(2) = COEF(2,JJ,MONTH)
      RJ = (TOD-1.)/3. - J + 1.
      DO 1 I=1,2
    1 A(I) = RJ*(B(I)-A(I)) + A(I)
C   THE ABOVE IS THE LINEAR INTERPOLATION IN TIME.
      XRAW = VEND(E,A)
      RETURN
      END
```

```
      FUNCTION VEND(END,A)
      DIMENSION A(2)
C  THIS IS THE INVERSE TRANSFORMATION.
C  A CONTAINS THE COEFFICIENTS.
      G = (END-A(1))/A(2)
      VEND = (EXP(G) - 244.)/1000.
C  METERS ARE CONVERTED TO KILOMETERS.
      IF(VEND.LT.0.) VEND = 0.
      IF(VEND.GT.30.) VEND = 30.
      RETURN
      END
```

b. Library Routines

ABS(X) provides absolute value of X.

AMOD(A,B) provides the remainder of A divided by B.

SECOND(X) provides current computer clock time and stores it in X. This value is used to seed the random number generator.

RANSET(X) initializes RANF with the random number seed, X.

RANF(X) provides random numbers of equal probability over the interval 0 to 1.

EXP(X) provides e^X.

SQRT(X) provides the square root of X.

c. Examples

Example 1: Generate 10 independent, randomly selected observations valid at 1230L in September.

```
      DO 2 I=1,10
    2 V(I) = PAWSES(-12.5,0.,9)
```

Example 2: Generate 10 observations in a sequence in which the first observation, valid at 0730L in October,

is randomly selected; the second observation is valid at 0900L; and subsequent observations are taken at two hour intervals.

```
      V(1) = PAWSES(-7.5,0.,10)
      V(2) = PAWSES(1.5,0.,10)
      DO 2 I=3,10
    2 V(I) = PAWSES(2.,0.,10)
```

Example 3: Generate two sequences of hourly observations, initiated at 0600L in November, wherein the initial value of the first sequence is 3 km and the initial value of the second sequence is chosen at random. This requires some computation by the user. Using the data within the array COEF in FUNCTION XRAW, the 0600L November coefficients require linear interpolation between the 0400L coefficients, COEF(I,2,11), and the 0700L coefficients, COEF(I,3,11), for I = 1, 2. The result is:

$$A(1) = -5.0398$$

$$A(2) = .571$$

then

$$END = A(2)\ \ln(v+\epsilon) + A(1)$$

where $v = 3000$ m and $\epsilon = 244$; thus END = -0.4216. The sequences are then generated as follows:

```
C  INITIAL VALUE IS 3 KM.
      RKIND = -20.4216
      V(1) = PAWSES(-6.,RKIND,11)
      DO 2 I=2,5
```

```
      2 V(I) = PAWSES(1.,0.,11)
C  RANDOM INITIAL VALUE.
        V(6) = PAWSES(-6.,0.,11)
        DO 3 I=7,10
      3 V(I) = PAWSES(1.,0.,11)
```

BIBLIOGRAPHY

BIBLIOGRAPHY

Boehm, A.R., 1976: Transnormalized Regression Probability. AWS-TR-75-259, Air Weather Service, Scott AFB, IL, 52 pp.

Boehm, A.R., and D.A. Abbott, 1977: The Air Weather Service environment simulation subroutine: A decision model component. Proceedings of the Summer Computer Simulation Conference, July 18-20, cosponsored by AMS, ISA, SCS, and SHARE, 11 pp.

Chisholm, D.A., and H. Kruse, 1974: The variability of visibility in the Hanscom mesonetwork: A preliminary assessment. Environmental Research Papers No. 479, AFCRL-TR-74-0265, AF Cambridge Research Laboratories.

Craig, R.A., 1965: The Upper Atmosphere: Meteorology and Physics. Academic Press, New York, 509 pp.

Feller, W., 1966: An Introduction to Probability Theory and Its Applications, Vol II. John Wiley & Sons, New York, 626 pp.

Fleagle, R.G., and J.A. Businger, 1963: An Introduction to Atmospheric Physics. Academic Press, New York, 346 pp.

Fleming, R.J., 1970: Concepts and Implications of Stochastic Dynamic Prediction. NCAR Cooperative Thesis # 22, University of Michigan and Laboratory of Atmospheric Science, NCAR.

Gringorten, I.I., 1966: A stochastic model of the frequency and duration of weather events. Journal Applied Meteorology, 5, pp 606-624.

Gringorten, I.I., 1976: Areal Coverage Estimates by Stochastic Modeling. AFGL-TR-76-0148, Environmental Research Papers, Air Force Geophysics Laboratory, Hanscom AFB, MA.

Klein, W.H., and H.R. Glahn, 1974: Forecasting local weather by means of model output statistics. Bull. Amer. Meteor. Soc., 55, pp 1217-1227.

Manabe, S., 1969: The atmospheric circulation and the hydrology of the earth's surface. Mon. Wea. Rev., 97, pp 739-774.

McCabe, J.T., 1968: Estimating conditional probability of events having marked diurnal variability. Proc. 1st Statistical Conf., Hartford, CT, Amer. Meteor. Soc., pp 163-172.

Miller, R.G., 1962: Statistical prediction by discriminant analysis. Meteorological Monographs, Vol 4, No 25, Amer. Meteor. Soc., Boston, MA, 54 pp.

Miller, R.G., 1964: Regression estimation of event probabilities. Tech Report 7411-121, Contract Cwb-10704, The Travelers Research Center, Inc., Hartford, Conn.

Miller, R.G., 1969: SLAM: A Screening Lattice Algorithm for Non-linear Regression Estimation of Event Probabilities. The Travelers Research Center, Inc., Hartford, Conn, 23 pp.

Pickett, K., T. Cassidy, and F. Campbell, 1977: (C) Simulating Combat Under Degraded Visibility (U), Tech Report TR 6-77, US Army Combined Arms Combat Developments Activity, US Army Night Vision Laboratories, US Army Material Systems Analysis Activity, 23 pp.

Savage, L.J., 1954: The Foundations of Statistics. John Wiley & Sons, Inc., New York, 150 pp.

Spiegel, M.R., 1975: Probability and Statistics. Schaum's outline series in mathematics, McGraw-Hill, 372 pp.

Shuman, F.G., and J.B. Hovermale, 1968: An operational six-layer primitive equation model. Jour. Appl. Meteor., 7, pp 525-547.

Tahnk, W.R., 1975: Objective prediction of fine scale variations in radiation fog intensity. AFCRL-TR-75-0169, AF Surveys in Geophysics No 311, Air Force Cambridge Research Lab., 37 pp.

Von Luetzow, H.B., 1973: Methods and Results of Remote Barometric Altimetry and Views on the Estimation of Meteorological Field Variables. Research Note ETL-RN-73-3, US Army Engineer Topographic Labs., Fort Belvoir, VA.

Whiton, R.C., 1977: Markov processes. AWS-TR-77-273, Selected Topics in Statistical Meteorology, Air Weather Service, Scott AFB, IL, pp 7-1 to 7-45.